



Single crystal studies on boron-rich τ -borides $\text{Ni}_{23-x}\text{M}_x\text{B}_6$ ($M = \text{Zn}, \text{Ga}, \text{In}, \text{Sn}, \text{Ir}$)—The surprising occurrence of B_4 -tetrahedra as a normal case?

Dominik Kotzott^a, Martin Ade^a, Harald Hillebrecht^{a,b,*}

^a Albert-Ludwigs-Universität Freiburg, Institut für Anorganische und Analytische Chemie, Albertstr. 21, D-79104 Freiburg, Germany

^b Freiburger Materialforschungszentrum FMF, Stefan-Maier-Str. 25, D-79104 Freiburg, Germany

ARTICLE INFO

Article history:

Received 23 May 2010

Received in revised form

28 July 2010

Accepted 31 July 2010

Available online 20 August 2010

Keywords:

Nickel borides

τ -borides

B_4 -tetrahedra

Single crystal growth

Structure analysis

XRD

EDX

ABSTRACT

Single crystals of the cubic τ -borides $\text{Ni}_{23-x}\text{M}_x\text{B}_6$ ($M = \text{Zn}, \text{Ga}, \text{In}, \text{Sn}, \text{Ir}$) were synthesised from the elements at temperatures between 1200 and 1500 °C. The structure refinements show that the existence of boron-rich phases is quite common. Starting from the idealised composition $\text{Ni}_{20}\text{M}'_3\text{B}_6$ a part of the metal atoms on site 8c is substituted by B_4 tetrahedra. For $M' = \text{Ga}$ a complete exchange seems to be possible leading to the composition $\text{Ni}_{20}\text{GaB}_{14}$. For $M' = \text{Zn}$ and Sn the formation of solid solutions is less extended. For $M' = \text{In}$ no exchange is observed but an unusual pattern of Ni/In distribution is observed. With $M = \text{Ir}$ mixed occupations occur for all sites and the boron content varies, too. All compositions were confirmed by EDX measurements.

© 2010 Elsevier Inc. All rights reserved.

1. Introduction

Metal rich borides of 3d transition metals with a $M:B$ ratio > 2 play an important role in hardening processes of alloys. They are formed on the surface by boridising (for example with gaseous BCl_3) or between the grain boundaries of the alloys by segregation. The so-called τ -borides with a composition $M_{23}\text{B}_6$ are the most numerous representatives of metal rich borides. Till date more than 80 representatives are known [1]. Its cubic crystal structure ($Fm\bar{3}m$) belongs to the Cr_{23}C_6 type [2], which contains 4 different metal sites (48h, 32f, 4a, 8c, see later). As pointed out by Stadelmeyer [3] τ -borides are typically ternary borides with a 3d-metal (Cr to Ni) on the sites 48h and 32f while the sites 4a and 8c are occupied by rare earth metals, 4d and 5d transition metals or a main group metal. Until 2009 binary τ -borides were assumed to exist only as metastable phases (first well-characterised example Co_{23}B_6 [4]) the minor component was called “ τ -stabiliser”. It was known that mixed occupation occurs for the different metal sites according to the different size [3–5] but usually a full occupation of the sites 4a and/or 8c is assumed to reach the ideal compositions $M_{22}M'B_6$, $M_{21}M'_2B_6$ and $M_{20}M'_3B_6$ with M' as τ -stabiliser.

Most of the investigations were done on powder samples for several reasons. Firstly τ -borides were usually investigated in the course of equilibrium studies. For this the samples were heated up for a short time near the assumed melting point and then annealed at temperatures between 800 and 1000 °C [3,5]. The resulting products were normally characterised only by metallographic methods and X-ray powder diffraction. Secondly the formation of single crystals is difficult because of kinetic reasons as melting points and annealing temperatures were very different. Therefore only a few detailed investigations of the formation of solid solutions in τ -borides on the basis of single crystal data are reported [1].

A new aspect started up, when it was shown for the τ -borides of the system $\text{Ni}/\text{Al}/\text{B}$ [6] that the enlargement of the boron content is caused by the substitution of aluminium on site 8c by B_4 -tetrahedra. It was the first example for a B_4 -tetrahedron in a typical solid state compound. Besides this there is also a mixed occupation of site 4a by Al and Ni. Therefore the formation of solid solutions is described by two different mechanisms: $\text{Ni}_{20}(\text{Al}_{1-x}\text{Ni}_x)(\text{Al}_{1-y}\text{B}_y)_2\text{B}_6$. (x, y between 0 and 1). Representatives are $\text{Ni}_{20.5}\text{Al}_{2.5}\text{B}_6$ ($a = 10.486 \text{ \AA}$, $x = 0.5$; $y = 0$), $\text{Ni}_{20}\text{Al}_3\text{B}_6$ ($a = 10.511 \text{ \AA}$, $x = y = 0$) and $\text{Ni}_{20}\text{AlB}_{14}$ ($a = 10.617 \text{ \AA}$, $x = 0$, $y = 1$). The enlargement of the lattice parameter with rising B-content is explained by the higher volume of a B_4 -tetrahedron in comparison to a single Al atom. Besides the use of excess Al played a central role for the formation and crystallisation of the boron-rich τ -boride.

In continuation of this work we have investigated other τ -borides of nickel, i.e. $M' = \text{Zn}, \text{Ga}, \text{In}$ and Sn concerning the

* Corresponding author at: Albert-Ludwigs-Universität Freiburg, Institut für Anorganische und Analytische Chemie, Albertstr. 21, D-79104 Freiburg, Germany. Fax: +49 761 203 6012.

E-mail address: harald.hillebrecht@ac.uni-freiburg.de (H. Hillebrecht).

formation of boron-rich phases. The special role of Ir-containing τ -phases was known from previous work [4,5,7] and therefore the system Ni/Ir/B was studied, too. Because the differences of the diffraction patterns are very small, the use of single crystal data is essential for unambiguous results. It turned out that in Ni-containing τ -borides two other main group metals ($M' = \text{Ga}, \text{Sn}$) are able to stabilise boron-rich τ -phases with B_4 -tetrahedra [8,9]. Furthermore, it was shown that iridium can substitute larger amounts (i.e. $x > 3$) of the 3d-metal ($\text{Cr}_{7.9}\text{Ir}_{14.1}\text{B}_6$ [7], $\text{Fe}_{10.0-15.4}\text{Ir}_{13.0-7.6}\text{B}_6$ [5]) and additionally, forms a boron-rich τ -boride ($\text{Ni}_{12.3}\text{Ir}_{8.7}\text{B}_{10.4}$).

2. Experimental

2.1. Syntheses and characterisation

The elements were mixed in ratios, which covers different amount of M' and boron. They were pressed into pellets (mass: ~ 300 mg) and put into a corundum crucible. Under an atmosphere of argon the pellets were heated up to a maximum temperature (1200–1450 °C) followed by a dwell time of several hours (1–10 h) and cooling down (rate: 10–15 °C/h) to a medium temperature (600–1000 °C). Then the furnace was turned off. Further investigations were done with the crushed metallic reguli. A few syntheses in the system Ni/Sn/B were done with an arc melter. Table 1 gives an overview on the synthesis of some typical samples. Because τ -borides were in the focus of interest compositions are usually given in a way that the amounts of Ni and M in the stoichiometric formula sum up to 23 and boron is between 6 (boron-poor) and 15 (boron-rich).

Powdered samples were characterised by XRD (STOE, Darmstadt, Germany, STADI-P, transmission geometry; $\text{MoK}\alpha$ -radiation and linear position sensitive detector (PSD) or $\text{CuK}\alpha$ -radiation and image plate (IP) detector). Silver metallic single crystals were collected from the crushed ingots as irregular polyhedral. Most of the single crystal investigations and data collections were performed by using a single crystal diffractometer equipped with an image plate detector (STOE, Darmstadt, Germany, IPDS II, $\text{MoK}\alpha$ -radiation, graphite monochromator). Measurements for the Sn-containing crystals were done with a conventional 4-circle diffractometer (Nonius, CAD4, $\text{MoK}\alpha$ -radiation, graphite monochromator). All measurements were done at room temperature. A numerical absorption correction was applied. For the IPDS data we used the equivalent method (Program XSHAPE [10]), for the CAD4 data the Psi-scan method.

The metal content was determined by the energy dispersive X-ray spectroscopy EDX (Electron microscope: Zeiss DSM-960; EDX-system: Link/LEO 1525). This was necessary for $M = \text{Ga}$ and Zn because of the similar electron numbers. For $M = \text{Ir}$ it was done because of the dissipation on all sites. Measurements were usually made of the crystals which were already used for the structure determinations (see later). Comparing compounds with known composition the errors can be estimated to be $\pm 1-2$ at%, depending on the quality of the surface and the elements involved. In contrast to several other cases (for example $\text{Li}_2\text{B}_{12}\text{C}_2$ [11], $\text{MgB}_{12}\text{C}_2$ [12], $\text{MgB}_{12}\text{Si}_2$ [13]) the unfavourable crystal shape prevented to obtain reliable data for the boron content.

2.2. Syntheses and experimental results

2.2.1. Ni/Ga/B

The formation of τ -phases occurs in a quite broad field of compositions. The access to single phase samples is possible. By-products are the binary Ni-borides, Ni-Ga alloys and the recently described ternary compound $\text{Ni}_{12}\text{GaB}_8$ [14]. The Ga-content can

vary between 5 and 15 at%. Remarkable is the variation of the boron content between 20 and 35 at%. With increase in the B-content the lattice parameter rises from $a = 10.50$ to 10.60 Å.

2.2.2. Ni/Zn/B

Because of the low boiling point of Zn the samples were welded in Ta-ampoules. Single phase τ -borides were obtained for boron-poor compositions ($a = 10.52-10.57$ Å). With higher boron content the amount of binary Ni-borides increased. Then the τ -phase was only a by-product and the lattice parameter could not be refined.

2.2.3. Ni/Sn/B

τ -phases as main products were obtained from boron-poor samples. A nearly single phase sample with small amounts of Ni resulted from a composition $\text{Ni}_{21}\text{Sn}_2\text{B}_6$ ($a = 10.585-10.587$ Å). With increase in the boron-content binary Ni-borides were found. The use of an arc melter revealed similar results.

2.2.4. Ni/In/B

The formation of a τ -boride was only observed for boron-poor samples. Single phase samples were obtained for compositions between $\text{Ni}_{22}\text{InB}_6$ and $\text{Ni}_{21}\text{In}_2\text{B}_6$. Obviously boron-rich τ -phases do not exist.

2.2.5. Ni/Ir/B

τ -phases were only observed for boron-rich samples. Boron-poor batches contained the binary borides of Ir and Ni. The variation of the lattice parameter is quite small indicating similar Ni/Ir-ratios.

2.3. Single crystal investigations and refinements

Single crystals were isolated from the crushed melt and investigated with a single crystal diffractometer. The indexing routine revealed a face-centred cubic unit cell in each case. Lattice parameters (10.46–10.95 Å) and reflection conditions were characteristic for τ -borides. The data sets were corrected for absorption and merged in Laue-class $m\bar{3}m$. The subsequent refinements (Program SHELXL [15]) were started with the known structure model of a τ -boride (cubic, $Z = 4$, space group $Fm\bar{3}m$ —No. 225). Because mixed occupations were expected all site occupation factors were checked. Mixed occupations were considered, if the deviations were greater than triple of the (usually very small) standard deviations. For all systems several single crystals were measured leading to very similar results. The results of the most reliable refinements (R -values, standard deviations, residual electron densities) were used for the discussion. Further details are listed in Tables 2–4, or may be obtained from Fachinformationszentrum Karlsruhe, D-76344 Eggenstein-Leopoldshafen (Germany) (Fax: +49)724-808-666; e-mail: crysdata@fiz-karlsruhe.de) on quoting the registry numbers CSD-421820 ($\text{Ni}_{20}\text{Ga}_3\text{B}_6$), CSD-421819 ($\text{Ni}_{20.0}\text{Ga}_{1.6}\text{B}_{10.1}$), CSD-421823 ($\text{Ni}_{21.4}\text{Zn}_{1.6}\text{B}_6$), CSD-421821 ($\text{Ni}_{20.0}\text{Zn}_{2.4}\text{B}_{7.75}$), CSD-421825 ($\text{Ni}_{22.2}\text{In}_{0.8}\text{B}_6$), CSD-421826 ($\text{Ni}_{22.0}\text{In}_{1.0}\text{B}_6$), CSD-421824 ($\text{Ni}_{21.6}\text{In}_{1.4}\text{B}_6$), CSD-421817 ($\text{Ni}_{12.3}\text{Ir}_{8.7}\text{B}_{10.4}$), CSD-421818 ($\text{Ni}_{20.9}\text{Sn}_{1.9}\text{B}_{7.3}$), CSD-421822 ($\text{Ni}_{21.1}\text{Sn}_{1.9}\text{B}_6$)

Because of the fundamental importance of the refinements they will be discussed in more detail.

2.3.1. $\text{Ni}_{20}\text{Ga}_3\text{B}_6$

The refinement was done with Ni on the sites of $M1$ and $M2$ and Ga on sites $M3$ and $M4$ resulting in excellent R -values of $R_1 = 0.0171$ and $wR_2 = 0.0166$. Each occupation factor (*sof*) was separately checked. The deviations from a complete and ordered occupation were very small. Furthermore, the displacement parameters are very similar indicating a correct assignment.

Table 1

Typical experimental conditions and results of XRD characterisation of τ -borides Ni/M/B (M =Ga, Zn, In, Sn, Ir), main part in **bold**; >, by-products; >>, traces; ?, not identified; –, not observed.

System/sample composition	Maximum temperature/holding time	Cooling rate	Lower holding temperature	τ -phase, powder	τ -phase single crystal	By-products
Ni/Ga/B						
Ni ₂₀ Ga ₃ B ₆	1450 °C/10 h	10 °C/h	1000 °C	10.5090(9)	10.4911(16)	>> Ni ₃ Ga
Ni ₂₀ Ga ₃ B ₁₂	1450 °C/10 h	10 °C/h	1000 °C	10.5886(11)	10.5434(18)	–
Ni ₂₀ Ga ₁ B ₁₂	1450 °C/10 h	10 °C/h	1000 °C	10.5886(8)	10.5528(13)	Ni ₂ B, Ni ₁₂ GaB ₈
Ni ₂₀ Ga _{0.5} B ₁₂	1450 °C/10 h	10 °C/h	1000 °C	10.5917(7)	–	Ni₂B
Ni ₂₀ Ga ₆ B ₁₂	1450 °C/10 h	10 °C/h	1000 °C	–	–	NiGa, Ni₂B
Ni ₂₀ Ga ₂ B ₁₅	1450 °C/10 h	10 °C/h	1000 °C	10.594(3)	–	Ni₂B
Ni ₂₀ Ga ₂ B ₁₂	1450 °C/10 h	10 °C/h	800 °C	10.583(3)	–	Ni₂B
Ni ₂₀ GaB ₁₂	1450 °C/10 h	10 °C/h	800 °C	10.5912(11)	–	Ni ₂ B, NiGa
Ni/Zn/B						
Ni ₁₈ Zn ₅ B ₆	1450 °C/1 h	20 °C/h	1000 °C	10.5716(5)	–	–
Ni ₁₉ Zn ₄ B ₆	1450 °C/1 h	20 °C/h	1000 °C	10.5642(2)	–	–
Ni ₂₁ Zn ₂ B ₆	1450 °C/1 h	20 °C/h	1000 °C	10.5221(9)	10.5409(17)	Ni ₃ B
Ni ₂₀ Zn ₃ B ₈	1450 °C/1 h	20 °C/h	1000 °C	10.54	10.5521(17)	Ni₃B
Ni ₂₀ Zn ₃ B ₁₀	1450 °C/1 h	20 °C/h	1000 °C	10.54	–	Ni₂B
Ni ₂₀ Zn ₃ B ₁₄	1450 °C/1 h	20 °C/h	1000 °C	–	–	o-Ni₄B₃ , NiB, Ni ₃ B
Ni/Sn/B						
Ni ₂₈ Sn ₂ B ₆	1450 °C/1 h	300 °C/h	800 °C	10.5853(3)	10.5827(3)	Ni
Ni ₂₅ Sn ₂ B ₆	1450 °C/1 h	300 °C/h	800 °C	10.5871(4)	–	Ni
Ni ₂₁ Sn ₂ B ₈	1450 °C/1 h	300 °C/h	800 °C	10.6056(8)	10.5958(3)	Ni ₂ B, <i>t</i> -Ni ₃ Sn ₂
Ni ₂₀ Sn ₃ B ₈	1450 °C/1 h	20 °C/h	1000 °C	10.6129(6)	–	<i>t</i> -Ni ₃ Sn ₂
Ni ₂₀ Sn ₃ B ₁₀	1450 °C/1 h	20 °C/h	1000 °C	10.6098(7)	–	Ni ₂ B, Ni ₃ Sn ₂
Ni ₂₁ Sn ₂ B ₆	Arc melting	–	–	10.5918(11)	–	–
Ni ₂₀ Sn ₃ B ₆	Arc melting	–	–	10.6045(2)	–	<i>h</i> -Ni ₃ Sn ₂
Ni ₂₁ SnB ₁₀	Arc melting	–	–	10.6065(13)	–	Ni₂B
Ni ₂₁ Sn _{0.5} B ₁₂	Arc melting	–	–	10.5917(4)	–	Ni₂B , Ni ₃ B
Ni ₂₀ Sn _{1.5} B ₁₂	Arc melting	–	–	–	–	Ni₂B , <i>h</i> -Ni ₃ Sn ₂
Ni/In/B						
Ni ₁₉ In ₄ B ₆	1350 °C/1 h	20 °C/h	900 °C	10.595(2)	10.5906(25)	<i>h</i> -In ₃ Ni ₂
Ni ₂₀ In ₃ B ₆	1350 °C/1 h	20 °C/h	900 °C	10.591(2)	–	> <i>h</i> -In ₃ Ni ₂
Ni ₂₁ In ₂ B ₆	1350 °C/1 h	20 °C/h	900 °C	10.578(1)	–	–
Ni ₂₂ In ₁ B ₆	1350 °C/1 h	20 °C/h	900 °C	10.550(4)	10.5412(18)	–
Ni _{17.25} In _{5.75} B ₆	1350 °C/1 h	20 °C/h	900 °C	10.590(2)	10.5951(15)	<i>h</i>-In₃Ni₂ , Ni ₂ B
Ni ₁₉ In ₄ B ₈	1350 °C/1 h	20 °C/h	900 °C	10.585(3)	–	<i>h</i> -In ₃ Ni ₂ , Ni ₂ B
Ni _{18.5} In _{4.5} B ₁₀	1350 °C/1 h	20 °C/h	900 °C	–	–	<i>h</i> -In ₃ Ni ₂ , Ni₂B , In
Ni/Ir/B						
Ni ₂₁ Ir ₂ B ₆	1450 °C/1 h	10 °C/h	1000 °C	–	–	Ni₂B , Ni ₃ – <i>x</i> Ir _{<i>x</i>} B
Ni ₁₇ Ir ₆ B ₆	1450 °C/1 h	10 °C/h	1000 °C	–	–	Ni₃B , Ni ₂ B, IrB _{1.1}
Ni ₁₃ Ir ₁₀ B ₆	1450 °C/1 h	10 °C/h	1000 °C	–	–	Ni₃–<i>x</i>Ir_{<i>x</i>}B
Ni _{14.5} Ir _{8.5} B ₁₅	1450 °C/1 h	10 °C/h	1000 °C	10.9366(13)	–	Ir
Ni _{13.5} Ir _{9.5} B ₁₅	1450 °C/1 h	10 °C/h	1000 °C	10.980(2)	10.9393(13)	NiB, Ni ₂ B, IrB _{1.1}
Ni _{11.5} Ir _{11.5} B ₁₅	1450 °C/1 h	10 °C/h	1000 °C	10.982(3)	–	<i>o</i> -Ni ₄ B ₃ , IrB _{1.1}
Ni _{9.5} Ir _{13.5} B ₁₅	1450 °C/1 h	10 °C/h	1000 °C	10.976(5)	–	IrB _{1.1}

The final difference Fourier synthesis shows no significant residual electron density. The electron numbers of Ni and Ga have a difference of 10%. Accordingly the exchange of Ga by Ni enlarges the *sof*-values to 110% (*M3*) and 113% (*M4*). A substitution of Ni1 and Ni2 by Ga is very unlikely because it demands the formation of short Ga–B bonds. Furthermore, it was not observed in the system Ni/Al/B.

2.3.2. Ni₂₀Ga_{1.6}B_{10.1}

With a structure model of a “regular” τ -boride Ni₂₀Ga₃B₆ the *R*-values are $R_1=0.13$ and $wR_2=0.26$. The displacement parameter of Ga on site 8c is enlarged by a factor 4. With a free site occupation factor the *sof*-value is reduced to 27(1)% and *R*-values of $R_1=0.031$ and $wR_2=0.056\%$. After this there remains a residual electron density of $3.5 e^-/\text{\AA}^3$ on a site $32f\ x,x,x$ with $x=0.194$ as it was known for boron-rich τ -borides [4,6]. With a partial occupation of this site by boron an occupation of 51(5)% is obtained and the *R*-values are again significantly reduced ($R_1=0.0185$, $wR_2=0.0302$). The composition determined by EDX was in excellent agreement (7.5 at% Ga: Ni_{21.25}Ga_{1.75}B₉).

These findings were confirmed for several single crystals from boron-rich batches with lattice parameters around 10.55 Å. Unfortunately, we were not able to obtain single crystals with the largest lattice parameters of 10.60 Å as it was refined from the powder XRD data. Similar to the τ -borides in Ni/Al/B we expect a complete substitution of Ga by B₄-tetrahedra and a composition Ni₂₀GaB₁₄.

2.3.3. Ni_{21.4}Zn_{1.6}B₆

According to the EDX results the crystal had a Ni:Zn ratio of 93:7. The refinement of the regular structure of a τ -boride with Zn on site 4a (i.e. Ni₂₂ZnB₆) resulted in *R*-values of $R_1=0.037$ and $wR_2=0.091$. The displacement parameter of *M3* was slightly enlarged (~40%) while that of *M4* (i.e. Zn) was comparable to Ni1 and Ni2. With a free *sof* of *M3* refined as *M*=Ni the occupation is reduced to 92(2)% and the *R*-values decrease to $R_1=0.036$ and $wR_2=0.089$. A share of 7% Zn (EDX) gives the composition Ni_{21.4}Zn_{1.6}B₆. Therefore additional Zn is expected which is probably located on *M3* (ca. 25%). On the other hand this was ignored in the refinement. A clear separation between *M*-deficit

Table 2Data for crystal structure analyses of τ -borides Ni/M'/B (M' =Zn, Ga, In, Sn, Ir), esd's in parentheses.

Compound	Ni ₂₀ Ga ₃ B ₆	Ni ₂₀ Ga _{1.6} B _{10.1}	Ni _{21.4} Zn _{1.6} B ₆	Ni ₂₀ Zn _{2.4} B _{7.75}	Ni _{22.2} In _{0.8} B ₆	Ni _{22.0} In _{1.0} B ₆	Ni _{21.6} In _{1.4} B ₆	Ni _{12.3} Ir _{8.7} B _{10.4}	Ni _{20.9} Sn _{1.8} B _{7.25}	Ni _{21.1} Sn _{1.9} B ₆
Crystal shape	Irregular fragment	Irregular fragment	Irregular fragment	Irregular fragment	Irregular fragment	Irregular fragment	Irregular fragment	Irregular fragment	Irregular fragment	Irregular fragment
Size in (mm ³)	0.01 × 0.02 × 0.02	0.02 × 0.03 × 0.02	0.02 × 0.02 × 0.01	0.04 × 0.04 × 0.04	0.01 × 0.01 × 0.01	0.02 × 0.02 × 0.02	0.03 × 0.03 × 0.03	0.01 × 0.01 × 0.01	0.02 × 0.02 × 0.03	0.02 × 0.03 × 0.02
Unit cell, <i>a</i> (Å)	10.4911(16)	10.5434(18)	10.5409(17)	10.5521(17)	10.5951(15)	10.5906(25)	10.5412(18)	10.9323(13)	10.5958(3)	10.5827(3)
Volume, <i>V</i> [Å ³]	1154.7(2)	1172.0(3)	1171.4(3)	1174.9(3)	1189.4(3)	1187.8(3)	1171.3(3)	1306.6(3)	1189.6	1185.2
<i>d</i> _{calc} [g/cm ³]	8.331	7.879	8.086	7.987	8.142	8.227	8.463	12.777	8.478	8.584
	0° ≤ ω ≤ 180°	0° ≤ ω ≤ 180°	0° ≤ ω ≤ 180°	0° ≤ ω ≤ 180°	0° ≤ ω ≤ 180°	0° ≤ ω ≤ 90°	0° ≤ ω ≤ 180°	0° ≤ ω ≤ 180°	Ω/2θ-scan	Ω/2θ-scan
	ψ=0°, 111; Δω=2°	ψ=0°, 111; Δω=2°	ψ=0°, 111; Δω=2°	ψ=0°, 111; Δω=2°	ψ=0°; Δω=2°	ψ=0°; Δω=2°	ψ=0°, 111; Δω=2°	ψ=0°, 111; Δω=2°	0.70° ± 0.40 tan θ	0.70° ± 0.40 tan θ
Exposure time (s)	300	300	300	180	900	180	180	300	90	90
Theta range	6.7° < 2θ < 65°	3° < 2θ < 69.8°	3° < 2θ < 65°	6.7° < 2θ < 65.8°	6.7° < 2θ < 67.6°	6.7° < 2θ < 65°	6.7° < 2θ < 65°	6.7° < 2θ < 64.8°	4° < 2θ < 80°	4° < 2θ < 80°
	-15 < <i>h</i> < 15	-16 < <i>h</i> < 16	-14 < <i>h</i> < 14	-16 < <i>h</i> < 16	-16 < <i>h</i> < 16	-16 < <i>h</i> < 16	-16 < <i>h</i> < 16	-16 < <i>h</i> < 16	-19 < <i>h</i> < 0	-19 < <i>h</i> < 0
	-15 < <i>k</i> < 15	-16 < <i>k</i> < 16	-14 < <i>k</i> < 14	-16 < <i>k</i> < 16	-16 < <i>k</i> < 16	-16 < <i>k</i> < 16	-16 < <i>k</i> < 16	-16 < <i>k</i> < 16	-19 < <i>k</i> < 0	-19 < <i>k</i> < 0
	-15 < <i>l</i> < 15	-16 < <i>l</i> < 16	-14 < <i>l</i> < 14	-16 < <i>l</i> < 16	-16 < <i>l</i> < 16	-16 < <i>l</i> < 16	-16 < <i>l</i> < 16	-16 < <i>l</i> < 16	-19 < <i>l</i> < 0	-19 < <i>l</i> < 0
μ (mm ⁻¹)	38.54	34.67	36.62	35.86	35.64	35.77	36.41	105.7	36.39	36.43
<i>R</i> _{int} / <i>R</i> _{sigma}	0.053/0.068	0.117/0.109	0.130/0.054	0.0685/0.046	0.129/0.054	0.0774/0.0273	0.094/0.048	0.174/0.077	0.0856/0.0498	0.0615/0.0371
<i>T</i> _{min} / <i>T</i> _{max}	0.282/0.524	0.200/0.395	0.191/0.398	0.015/0.056	0.017/0.061	0.027/0.078	0.017/0.064	0.0045/0.048	0.115/0.213	0.056/0.084
<i>N</i> (<i>hkl</i>) meas.; unique	6576, 137	6613, 160	5622, 118	6046, 135	5595, 151	1274, 134	6412, 135	6389, 144	1040, 223	1040, 224
<i>N</i> (<i>hkl</i>) (<i>I</i> > 2σ(<i>I</i>))	87	133	97	94	114	102	86	108	193	182
Param. refined	14	18	15	16	15	15	14	16	16	16
<i>R</i> ₁ (<i>F</i>)/ <i>wR</i> ₂ (<i>F</i> ²)	0.0171/0.0166	0.0182/0.0297	0.0357/0.0889	0.0119/0.0125	0.0489/0.0770	0.0201/0.0295	0.0283/0.0401	0.0206/0.0224	0.0193/0.0365	0.0165/0.0294
<i>R</i> ₁ (<i>F</i>), all data	0.0380	0.0247	0.0411	0.0249	0.066	0.0300	0.0466	0.0366	0.0273	0.0281
Weighting scheme	0.0/0.0	0.0146/0.0	0.0618/3.19	0.0/0.0	0.021/630.0	0.0088/0.0	0.013/0.0	0.0/0.0	0.0/0.0	0.0046/0.0
[15]										
Extinction [15]	0.00021(1)	0.0018(1)	0.0005(2)	0.00024(1)	0.00025(7)	0.00128(6)	0.00000(3)	0.00076(3)	0.0019(1)	0.0014(1)
Goodness of fit	0.446	0.449	1.056	0.559	1.200	1.066	0.852	0.588	0.978	1.022
Residual electron density in [e ⁻ /Å ³]	+0.75/-0.70	+0.86/-1.06	+0.95/-0.99	+0.36/-0.36	+1.38/-3.25	+1.11/-0.77	+1.05/-1.52	+2.36/-2.11	+1.06/-1.03	+0.90/-1.11
(max, min, σ)	0.16	0.19	0.28	0.10	0.36	0.18	0.26	0.33	0.25	0.23

Table 3Coordinates, displacements parameters and occupation factors of τ -borides Ni/M'/B ($M' = \text{Zn, Ga, In, Sn, Ir}$).

Compound	Ni ₂₀ Ga ₃ B ₆	Ni _{20.9} Ga _{1.6} B _{10.1}	Ni _{21.4} Zn _{1.6} B ₆	Ni ₂₀ Zn _{2.4} B _{7.75}	Ni _{22.2} In _{0.8} B ₆	Ni _{22.0} In _{1.0} B ₆	Ni _{21.6} In _{1.4} B ₆	Ni _{12.3} Ir _{8.7} B _{10.4}	Ni _{20.9} Sn _{1.8} B _{7.25}	Ni _{21.1} Sn _{1.9} B ₆
Ni1, site 32f (x,x,x)										
<i>x</i>	0.38228(4)	0.38027(4)	0.38287(11)	0.38242(3)	0.38418(14)	0.38467(6)	0.38486(9)	0.37617(4)	0.38457(2)	0.38503(2)
<i>U</i> _{eq}	0.0071(2)	0.0095(2)	0.0168(6)	0.0151(1)	0.0206(6)	0.0112(3)	0.0161(4)	0.0048(2)	0.0066(1)	0.0069(1)
sof Ni, ratio Ni/M	98.4(5) ^a	100.6(5) ^a	98.7(13) ^a	99.7(6) ^a	100.0(15) ^a	101.0(7) ^a	98.4(11) ^a	15.8(5)/84.2 ^b	100.2(4) ^a	100.0(3) ^a
<i>U</i> ₁₁ = <i>U</i> ₂₂ = <i>U</i> ₃₃	0.0095(2)	0.0095(2)	0.0168(6)	0.0151(1)	0.0206(6)	0.0117(3)	0.0161(4)	0.0047(2)	0.0060(1)	0.0069(1)
<i>U</i> ₁₂ = <i>U</i> ₁₃ = <i>U</i> ₂₃	0.0008(2)	0.0017(2)	0.0012(4)	0.0022(1)	0.0067(6)	0.0044(3)	0.0015(4)	0.0008(1)	0.0023(1)	0.0007(1)
Ni2, site 48h (0,y,y)										
<i>y</i>	0.16923(4)	0.16924(4)	0.16979(9)	0.16994(3)	0.16958(11)	0.16923(5)	0.16994(3)	0.16539(7)	0.16895(2)	0.16873(2)
<i>U</i> _{eq}	0.0072(1)	0.0093(1)	0.0167(5)	0.0134(1)	0.0156(5)	0.0076(2)	0.0149(3)	0.0047(4)	0.0050(2)	0.0069(1)
sof Ni, ratio Ni/M	101.6(4) ^a	100.1(6) ^a	101.1(13) ^a	100.3(4) ^a	100.3(15) ^a	99.2(7) ^a	101.8(11) ^a	84.0(8)/18.0 ^b	100.3(2) ^a	99.5(4)
<i>U</i> ₁₁	0.0087(3)	0.0102(3)	0.0168(8)	0.0146(2)	0.0172(8)	0.0088(3)	0.0140(4)	0.0047(4)	0.0045(1)	0.0062(1)
<i>U</i> ₂₂ = <i>U</i> ₃₃	0.0065(2)	0.0089(2)	0.0166(6)	0.0127(1)	0.0148(5)	0.0070(4)	0.0165(4)	0.0049(5)	0.0060(1)	0.0084(1)
<i>U</i> ₂₃	0.0007(2)	0.0003(2)	0.0007(5)	0.0009(1)	0.0014(6)	0.0004(2)	−0.0007(4)	0.0000(2)	0.0004(1)	0.0003(1)
M3, site 8c (1/4,1/4,1/4)										
<i>U</i> _{iso}	0.0123(3)	0.0100(15)	0.0156(10)	0.0166(5)	0.0142(14)	0.0072(6)	0.0174(8)	0.0055(29)#	0.0065(1)#	0.0082(1)#
sof M, ratio Ni/M	97.0(8) ^a	26.8(8)	92.3(13) (Ni)	68.5(6) ^a (Zn)	85(4)/15(4) ^b	80(3)/20(3) ^b	31(3)/69(3) ^b	65.8(4) (Ni)	85.8(4) ###	7.0(7)/93.0
M4, site 4a (0,0,0)										
<i>U</i> _{iso}	0.0090(5)	0.0119(4)	0.0156(10)	0.0136(3)	0.0161(19)	0.0074(10)	0.0150(10)	0.0055(29)#	0.0050(3)#	0.0085(4)#
sof M, ratio Ni/M	99.9(17) ^a	96.7(13) ^a	97.5(25) ^a	99.2(11) ^a	54(6)/46(6) ^a	60(2)/40(2) ^b	98(3) ^a	17.8(17) (Ni)	14.4(11)/85.6 ^b	95.6(10)/4.4 ^b
B1, site 24e (0,0,z)										
<i>z</i>	0.2765(8)	0.2782(8)	0.2744(19)	0.2763(6)	0.2770(23)	0.2739(9)	0.2755(16)	0.2793(20)	0.2714(4)	0.2714(4)
<i>U</i> _{eq} / <i>U</i> _{iso}	0.0060(14)	0.0120(11)	0.0205(37)	0.0174(9)	0.0189(38)	0.0062(15)	0.0147(27)	0.01 fixed	0.0060(5)###	0.0080(6)###
sof	103(5) ^a	88(4) ^a	114(7) ^a	107(2) ^a	89(11) ^a	90(5) ^a	96(8) ^a	102(7) ^a	101(2) ^a	101(2) ^a
<i>U</i> ₁₁ = <i>U</i> ₂₂	0.0067(18)	0.0146(16)	–	–	–	–	–	–	–	–
<i>U</i> ₃₃	0.0047(36)	0.0068(25)	–	–	–	–	–	–	–	–
B2, site 32f (x,x,x)										
<i>x</i>	–	0.1939(8)	–	0.1933(15)	–	–	–	0.1954(17)	0.1923(14)	–
<i>U</i> _{eq}	–	0.0206(48)	–	0.025 (fixed)	–	–	–	0.010 fixed	0.0060(5)###	–
sof	–	51(5)	–	21.7(16)	–	–	–	55(6)	14.2(4)###	–

#, ##, ### coupled refinement.

^a In order to check for mixed occupations and/or vacancies site occupation factors were treated by turns as free variables at the end of the refinement. For the discussion and the final refinement a full occupation is assumed.^b Refined as mixed occupation Ni/M ($M = \text{Ga, Zn, Sn, In, Ir}$), in sum a full occupation is assumed.

and Zn/Ni ratio is impossible. The residual electron density was featureless, especially of the 32f site.

2.3.4. Ni_{20.0}Zn_{2.4}B_{7.75}

The refinement with the ordered model of Ni₂₀Zn₃B₆ and completely occupied sites yielded *R*-factors of *R*₁=0.043 and *wR*₂=0.060. The displacement parameter of the Zn atom on the 8c site was three-times larger than the others. With a free site occupation factor the occupation decreased to 69% and the *R*-values to *R*₁=0.016 and *wR*₂=0.020. The maximum of the residual electron density was +1.2 e[−]/Å³ on a 32f-site with *x* ≈ 0.196. With boron on this site (free *sof*, displacement parameter fixed to 0.02) the refinement converged at *R*₁=0.0119 and *wR*₂=0.0125 and the residual electron density decreased significantly to +0.36 e[−]/Å³. The Ni/Zn ratio from the refinement is 89.4%/10.6%. This is close to the data obtained by EDX (88%/12%). The small deviation may result from a partial Ni-occupation of the sites 4a and 8c, but the difference between Ni and Zn is not sufficient for a separation.

2.3.5. Ni_{21.1}Sn_{1.9}B₆

The refinement with a completely ordered model, i.e. Sn on 8c and the composition Ni₂₁Sn₂B₆, resulted in *R*-values of *R*₁=0.018

and *wR*₂=0.036. The displacement parameters of Ni4 (4a) and Sn3 (8c) were slightly reduced and enlarged, respectively. Accordingly, the refinement with mixed occupations resulted in a small improvement (*R*₁=0.0165, *wR*₂=0.030). The residual electron density was featureless.

2.3.6. Ni_{20.0}Sn_{2.4}B_{7.75}

The refinement was started with the model of Ni₂₁Sn₂B₆. It turned out that the electron density is about 10% enlarged on site 4a and 14% reduced on site 8c. The introduction of mixed Ni/Sn occupations resulted in *R*-values of *R*₁=0.019 and *wR*₂=0.037. The highest residual electron density of +1.4 e[−]/Å³ was found for a 32f-site with *x* ≈ 0.195, slightly above the background. Because the crystal was from a boron-rich sample with enlarged lattice parameter we assumed a partial exchange of Sn by boron (7.6(14)%). Now the electron density map was “empty”. An additional substitution of Sn by Ni is possible but was not taken into account. According to the small exchange and the low electron number of boron the *R*-values are nearly unchanged.

2.3.7. Ni_{21.4}In_{1.6}B_{6N}

The refinement was started with the model of Adelsberger and Jansen [16], i.e. the composition Ni₂₁In₂B₆ and In on site 8c

Table 4Selected distances in τ -borides Co/M/B ($M = \text{Al, Ga, Sn, Ir}$), esd's in parentheses.

Compound	Ni ₂₀ Ga ₃ B ₆	Ni _{20.9} Ga _{1.6} B _{10.1}	Ni _{21.4} Zn _{1.6} B ₆	Ni ₂₀ Zn _{2.4} B _{7.75}	Ni _{22.2} In _{0.8} B ₆	Ni _{22.0} In _{1.0} B ₆	Ni _{21.6} In _{1.4} B ₆	Ni _{12.3} Ir _{8.7} B _{10.4}	Ni _{20.9} Sn _{1.8} B _{7.25}	Ni _{21.1} Sn _{1.9} B ₆
Ni1–B1 3x	2.069(5)	2.085(4)	2.087(11)	2.082(3)	2.074(13)	2.088(5)	2.068(9)	2.188(11)	2.105(2)	2.099(2)
Ni1–M3	2.4036(8)	2.3790(8)	2.426(2)	2.4203(6)	2.462(3)	2.4703(11)	2.4621(17)	2.3871(7)	2.4697(5)	2.4751(5)
Ni1–M1 3x	2.4701(10)	2.5247(9)	2.469(2)	2.4814(7)	2.454(2)	2.4428(13)	2.4275(19)	2.7074(8)	2.4462(5)	2.4334(5)
Ni1–M2 6x	2.6101(6)	2.6109(6)	2.623(1)	2.6214(5)	2.6458(13)	2.6502(6)	2.6410(10)	2.7074(8)	2.6528(2)	2.6540(2)
Ni1–B2 3x	–	2.255(2)	–	2.293(3)	–	–	–	2.265(3)	2.340(3)	–
Ni2–B1 2x	2.102(5)	2.122(4)	2.102(11)	2.115(3)	2.127(13)	2.107(5)	2.105(9)	2.195(13)	2.093(2)	2.090(2)
Ni2–M2	2.3966(14)	2.4086(11)	2.391(3)	2.3895(8)	2.410(3)	2.4194(15)	2.417(2)	2.5470(11)	2.4290(6)	2.4327(6)
Ni2–M2 4x	2.5109(8)	2.5234(7)	2.531(1)	2.5360(6)	2.5409(17)	2.5346(8)	2.5184(13)	2.5570(11)	2.5317(3)	2.5252(3)
Ni2–M4	2.5109(8)	2.5234(7)	2.531(1)	2.5360(6)	2.5409(17)	2.5346(8)	2.5184(13)	2.5570(11)	2.5317(3)	2.5252(3)
Ni2–M1 4x	2.6102(6)	2.6109(6)	2.623(1)	2.6214(5)	2.6458(13)	2.6502(6)	2.6410(10)	2.7071(5)	2.6528(2)	2.6540(2)
Ni2–M3 2x	2.8835(5)	2.8979(5)	2.8938(7)	2.8959(5)	2.9100(8)	2.9109(5)	2.8991(7)	3.0282(6)	2.9141(2)	2.9119(2)
Ni2–B2 2x	–	2.076(12)	–	2.069(19)	–	–	–	2.186(24)	2.067(18)	–
Ni3–M1 4x	2.4036(8)	2.3790(8)	2.426(2)	2.4203(6)	2.462(3)	2.4703(11)	2.4622(17)	2.3891(7)	2.4697(5)	2.4751(5)
Ni3–M2 12x	2.8835(5)	2.8979(5)	2.8938(7)	2.8959(5)	2.9100(8)	2.9109(5)	2.8991(7)	3.0282(6)	2.9141(2)	2.9119(2)
Ni3–B2 4x	–	1.027(16)	–	1.04(3)	–	–	–	1.04(3)	1.06(2)	–
Ni4–M2 12x	2.5109(8)	2.5234(7)	2.531(1)	2.5360(6)	2.5409(17)	2.5346(8)	2.5184(13)	2.5570(11)	2.5317(3)	2.5252(3)
B1–M1 4x	2.069(5)	2.085(4)	2.087(11)	2.082(3)	2.074(13)	2.088(5)	2.068(9)	2.188(11)	2.093(2)	2.090(2)
B1–M2 4x	2.102(5)	2.122(4)	2.102(11)	2.115(3)	2.127(13)	2.107(5)	2.105(9)	2.195(13)	2.105(2)	2.099(2)
B2–Ni3	–	1.025(14)	–	1.04(3)	–	–	–	1.04(3)	1.06(2)	–
B2–B2 3x	–	1.68(3)	–	1.69(4)	–	–	–	1.69(5)	1.73(4)	–
B2–M2 3x	–	2.076(12)	–	2.069(19)	–	–	–	2.186(24)	2.067(18)	–
B2–M1 3x	–	2.255(2)	–	2.26(2)	–	–	–	2.265(3)	2.340(3)	–

($R_1 = 0.042$, $wR_2 = 0.059$). The subsequent refinement with free *sof*'s resulted in small deviations as indicated by the displacement parameters and an amelioration of the *R*-values. While site 4a was only occupied by Ni, site 8c showed a mixed occupation with 69(3)% In ($R_1 = 0.028$, $wR_2 = 0.040$).

2.3.8. Ni_{22.0}In_{1.0}B₆

According to the increased In-content of the melt and the enlarged lattice parameter we expected a higher In-content on sites 4a and/or 8c. This was true for the 4a-site with 40(2)% In, but surprisingly the In-occupation on site 8c sank to 20(2)%. According to the residual electron density $+1.1 \text{ e}^-/\text{\AA}^3$ on the well-known 32*f*-site a small amount of additional boron might be possible, but the quality of the data allows no clear statement, so this is discarded. Final *R*-values are $R_1 = 0.020$ and $wR_2 = 0.0295$. The decrease in the In-content was also confirmed by EDX (Ni_{21.4}In_{1.6}B₆: 8%, Ni_{22.0}In_{1.0}B₆: 5%).

2.3.9. Ni_{22.2}In_{0.8}B₆

The results of the refinement were very similar to the previous one. In comparison to Ni_{22.0}In_{1.0}B₆ the In-content on 8c was further decreased and that of 4a increased. The resulting occupations by In were 54(6)% on site 4a and 15(4)% on site 8c. The higher *R*-values are caused by the crystal quality.

2.3.10. Ni_{12.3}Ir_{8.7}B_{10.4}

According to the composition for the synthesis (58.3% Ni, 41.7% Ir) and the value of the lattice parameter ($a = 10.932 \text{ \AA}$) we expected a partial occupation of the metal sites M1 and M2 by Ir. It turned out very soon that the electron density is by far the highest for M1, while it is reduced for M3 and M4. Therefore the refinement was done in a way that the ratio Ni:Ir on site M1 was fixed and the ratio on M2 refined as a free parameter. The sites M3 and M4 were assumed to be occupied by Ni and refined with free occupation factors. The ratio on M1 was changed stepwise until the total Ni–Ir ratio corresponded to the value which was determined for that crystal by EDX (58.4% Ni, 41.6% Ir). This procedure is not unambiguous, because in principle the sites M3

and M4 can be occupied by Ir, too. But according to the high symmetry (and the low multiplicity) this approximation has only a small influence on the overall composition, so we assumed an occupation solely by Ni. The boron site 24e can be derived from difference Fourier synthesis with a value of $+8.1 \text{ e}^-/\text{\AA}^3$. At that stage of the refinement there is a residual electron density of $+4.4 \text{ e}^-/\text{\AA}^3$ on a 32*f* site with $x = 0.192$, which is clearly higher than the background of $\pm 2 \text{ e}^-/\text{\AA}^3$. The occupation of this site by boron results in a *sof* of 55(6)%. To obtain a stable refinement the displacement parameters of boron were fixed. Finally, *R*-values of $R_1(F) = 0.014$ and $wR_2(F^2) = 0.023$ were obtained.

The general findings (mixed occupation of M1 and M2 with preference of M1 by Ir, partial occupations of M3 and M4, residual electron density on site 32*f*) were confirmed for several crystals from boron-rich samples.

3. Results and discussion

The crystal structure of τ -phases was first determined for Cr₂₃C₆ [2]. Boron or carbon has a quadratic antiprismatic coordination. The same coordination is found for the binary borides of those transition metals (Cr₂B, Mn₂B, Fe₂B, Co₂B, Ni₂B [1]), which are also the most frequent metals for τ -borides. Fig. 1 shows the crystal structure of a τ -phase with a special emphasis on the four different metal positions. It is built up by a cubic face-centred packing of cuboctahedra which are formed by the metal atoms M2 on site 48*h* and centred by the metals M4 on site 4a. The octahedral “voids” are filled by cubes of the metal atoms M1 on site 32*f* (M1) and the atoms M3 on site 8c occupy the tetrahedral “voids”. The quadratic antiprismatic coordination of the boron atoms is formed by the square planes of the cuboctahedra and the cubes. Coordination polyhedra are shown in Fig. 2.

In general the distances *M–M* and *M–B* correspond to the sum of the covalent radii (Ni: 1.25 Å, Zn: 1.34 Å, Ga: 1.35 Å, In 1.67 Å, Sn: 1.54 Å, Ir: 1.36 Å) [17] and are therefore not discussed in detail. The larger radius of Ir compared to Ni is clearly seen in the distances *M–B* and the corresponding *M–M* distances (M1–M1, M1–M2, M2–M2). An interesting feature is the surrounding M3

on site 8c which is usually occupied by the large metal atoms. 12 atoms M2 form a truncated tetrahedron (Friauf-polyhedron) with quite long distances, while the four hexagons of the

Friauf-polyhedron are capped by M1 with significantly shorter distances. This seems to be important for the substitution $M3 \leftrightarrow B_4$ -tetrahedron (see later).

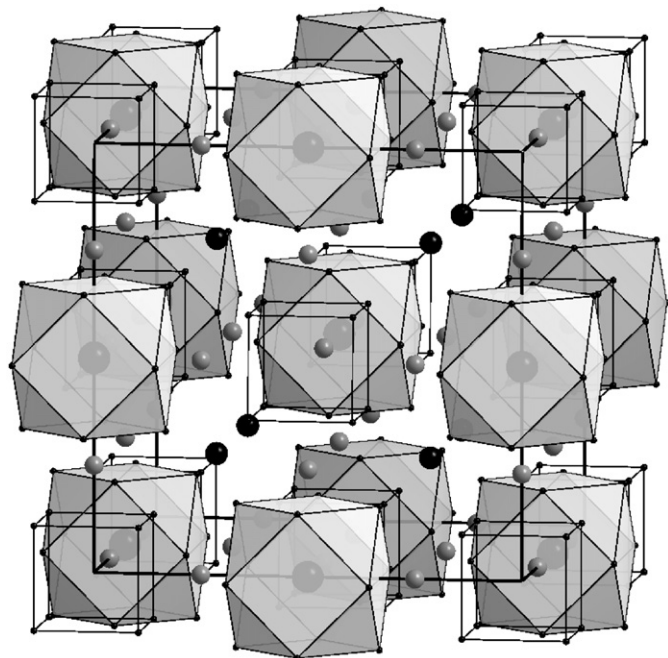


Fig. 1. Crystal structure of τ -Borides $M_{23}B_6$; M1: M_8 -cubes, M2: M_{12} -cuboctahedra centred by M3, isolated M-atoms: M4; grey circles: boron, black circles: metal atoms.

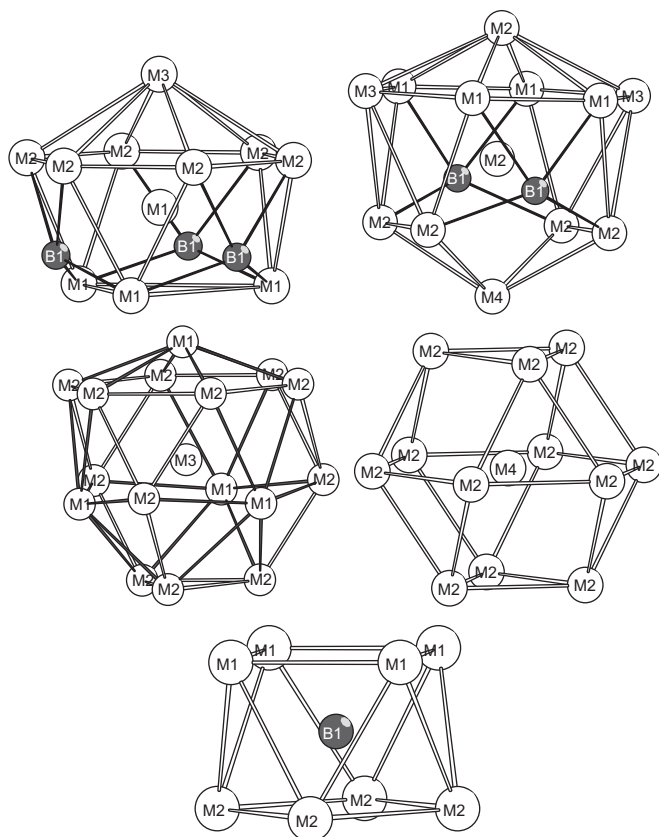


Fig. 2. Coordination polyhedra in τ -borides.

3.1. Ni/Ga/B

The system Ni/Ga/B was already investigated by Stadelmaier and Fiedler [18] and Chaban and Kuzma [19]. Both confirm the existence of a τ -boride. According to Stadelmaier it melts congruently. At 800 °C the stability extends to 21 at% boron and 6–12 at% gallium. The lattice parameters vary between 10.481 and 10.519 Å, Ga prefers the site 8c (i.e. $Ni_{21}Ga_2B_6$ with 8.7% Ga) and there is no boron-rich phase. Kuzma confirms composition ($Ni_{19.5}Ga_{3.5}B_6$) and lattice parameter (10.512 Å) but assumes a homogenous distribution of Ga.

Our results confirm the existence of boron-poor τ -boride with a lattice parameter around 10.50 Å and a composition $Ni_{20}Ga_3B_6$. The variation of the lattice parameter is clearly larger with an upper limit of 10.60 Å.

The refinement of the single crystal data with the shortest lattice parameter suggests a composition $Ni_{20}Ga_3B_6$ with Ga on both sites 4a and 8c, but small amount of Ni cannot be excluded. There is no significant occupation of M1 and M2 by Ga, in agreement to the very rare examples of Ga–B bonds [14] and the non-existence of binary Ga borides [1].

With increase in the boron content the lattice parameter rises up to a maximum of 10.60 Å (~ 33 at% B). The single crystal data clearly show a decrease in the electron density on site 8c and the additional density on site 32f ($x \approx 0.194$). The refinement indicates a partial substitution of Ga by B_4 -tetrahedra. The resulting Ni–B distances 2.08 Å are comparable to other binary Ni borides. The B–B distances of 1.68(3) Å within the tetrahedron are similar to molecules with B_4 -tetrahedra (B_4Cl_4 : 1.65 Å [20,21]; $(tBu)_4B_4$: 1.71 Å [22]) and other boron-rich τ -borides ($Ni_{20}AlB_{14}$: 1.68 Å, [6], $Co_{12.3}Ir_{8.9}B_{10.5}$: 1.63 Å [4]). The perfect fitting of the coordination around the 8c-site with symmetry $43m$ for a B_4 -tetrahedron is shown in Fig. 3.

In general, there is a strong analogy to the τ -borides of the system Ni/Al/B. Here, the substitution increases the lattice parameter from 10.511 Å for $Ni_{20}Al_3B_6$ to 10.617 Å for $Ni_{20}AlB_{14}$.

We did not obtain suitable single crystals with lattice parameters above 10.56 Å. This might be due to the conditions of crystallisation. We expect the interaction with a liquid phase (solution/flux) is essential to form single crystals of sufficient size. According to the results of the powder investigations the maximum of the lattice parameter is around 10.60 Å. Estimated from the increase in the volume by the substitution $Ga \rightarrow B_4$ the corresponding composition of the boron-rich phase is quite close to $Ni_{20}GaB_{14}$.

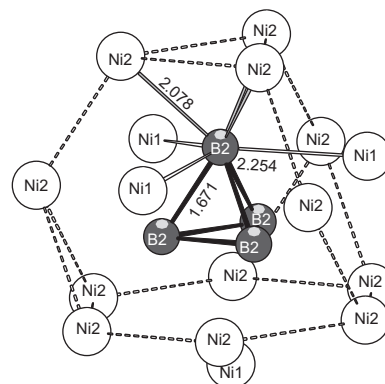


Fig. 3. Coordination of the B_4 -tetrahedron in $Ni_{20}Ga_{1.6}B_{10.1}$.

3.2. $Ni_{20.0}Zn_{2.4}B_{7.75}$

The existence of a τ -boride with Zn was already described by Stadelmaier et al. [23,24]. In the isothermal section at 800 °C they found an appreciable phase width of the τ -phase with lattice parameters between $a=10.498$ Å (72% Ni, 8% Zn, 20% B: $Ni_{20.3}Zn_{2.7}B_6$) and $a=10.555$ Å (63% Ni, 12% Zn, 25% B: $Ni_{19.3}Zn_{3.7}B_{7.25}$).

Our results are in excellent agreement with the results of Stadelmaier. The boron-poor single crystal ($a=10.541$ Å) shows nearly completely occupied metal sites on 4a and 8c and no significant residual electron density. In this case the reliability is limited because of the poorer crystal quality (see *R*-factors) and the unfortunate electronic situation (separation Ni/Zn, extent of additional boron).

For the single crystal from the boron-rich sample the occurrence of an additional residual electron density on a 32*f*-site is connected to a decrease in the electron density on site 8c and an enlargement of the lattice parameter. For the investigated single crystal the occupation by the B_4 -tetrahedra is about 20%. The distances Ni–B (2.07 Å) and B–B (1.69 Å) fit very well to the other τ -borides with B_4 -tetrahedra. But again the small difference of the electron numbers between Ni and Zn and the limited exchange of Zn by B_4 -tetrahedra reduce the reliability of the X-ray investigation.

3.3. Ni/Sn/B

The system Ni/Sn/B was investigated by Stadelmaier and co-workers in the 1960s [24–26]. They found the τ -boride as the only ternary compound with a small variation of the Sn-content (6.0–6.8 at%) and a larger one for boron (17.5–27.5 at%, i.e. $Ni_{21}Sn_2B_5$ – $Ni_{21}Sn_2B_9$). Lattice parameters were between 10.584 and 10.598 Å. Our results are in very good agreement. The variation of the boron content is explained by the substitution of Sn on site 8c by B_4 -tetrahedra. The distances (Ni–B: 2.07 Å, B–B: 1.73 Å) are comparable to the other systems with B_4 -tetrahedra. The substitution has only a little influence on the lattice parameter, because the volumes of B_4 -tetrahedra and Sn are comparable (see τ -borides Ni/Al/B). Therefore a statement on the upper limit of the substitution is difficult. According to the results of Stadelmaier it is about 20%.

3.4. Ni/In/B

The system Ni/In/B was investigated in detail by Schöbel and Stadelmaier [27] Stadelmaier and Yun [28]. Besides the perovskite-related compound $Ni_3InB_{0.5}$ they found at 800 °C a τ -boride with 20–24 at% boron. The In-content varied between 4 at% ($Ni_{21.8}In_{1.2}B_{5.8}$, $a=10.581$ Å) and 8 at%, ($Ni_{20.6}In_{2.4}B_7$, $a=10.609$ Å). The τ -phase with the composition $Ni_{21}In_2B_6$ melts congruently. Additionally, they observed at higher In-content the occurrence of two liquid phases, similar to the system Co/In/B [29–31]. In a recent contribution Adelsberger and Jansen [16] communicated a completely ordered structure of $Ni_{21}In_2B_6$ (i.e. In on site 8c) by refinement of single crystal data ($a=10.5911$ Å).

Our results for the refinements of the single crystal from an In-poor melt are in agreement with the work of Stadelmaier and Jansen. The lower limit of the In-content corresponds to a lattice parameter of about 10.55 Å (powder and single crystal), the smaller lattice parameter is explained by the partial occupation of site 8c by In.

The enlargement of the lattice parameter to $a \sim 10.60$ Å by increase in the In-content was expected, but surprisingly we observed a reduction of the single crystal's In-content because the increase of indium on site 4a is more than compensated by the

decrease on site 8c. The reason why indium now prefers the 4a site is not yet clear but the refinement indicates this without doubt.

The unexpected behaviour might be explained by a phase separation. The existence of two liquid phases was already described by Stadelmaier, who had investigated the solidified melts by metallography. The binary diagram Ni/In performs several different binary alloys between the compositions In_3Ni_2 and Ni_2In , which all solidify around 900 °C [32]. The compositions in our experiments were chosen in a way that there is an excess of In with respect to the stable τ -phase. Therefore the coexistence of two liquid phases around the temperature of the crystal growth of the τ -phase is possible. This might explain, too, why we observe In_3Ni_2 as an In-rich intermetallic phase in the solidified regulus.

The increase in the cell volume with the increase in Ni-content is puzzling because of the bigger size of In (r_{In} : 1.67 Å; r_{Ni} : 1.28 Å [17]). The calculation of the valence sum according to the method of Brown [33] shows that the efficient size of the coordination sphere for *M3* is larger than for *M4*. With the parameters of $Ni_{22}InB_6$ one obtains a valence sum of 7.84 for *M3* and of 5.94 for *M4*. Therefore one would expect that large metal atoms like Al, Ga, Sn and In are preferentially located on site 8c. This is true for most of the examples, but not for the τ -borides grown from an In-rich melt. Nevertheless, it explains, why the lattice parameter is enlarged despite the lower In content. Additionally, it corresponds to the longer distances *M4*–Ni2 in $Ni_{22.2}In_{0.8}B_6$ and $Ni_{22.0}In_{1.0}B_6$ and the shorter ones in $Ni_{21.6}In_{1.4}B_6$.

It should be mentioned that the τ -borides of the system Co/In/B play a special role, too. The binary $Co_{23}B_6$ was grown from an In-melt and there is a miscibility gap of the liquid phases [29–32].

3.5. $Ni_{12.3}Ir_{8.7}B_{10.4}$

Till date there were no investigations on the ternary system Ni/Ir/B. The tendency of Ir to form τ -borides with a very high Ir-content was well-known [4,5,7,34]. Furthermore, it was known that τ -borides of Ni form extended solid solutions with platinum metals ($Ni_{23-x}Re_xB_6$, $x=10$ –13 [35]). Finally, the substitution of B_4 -tetrahedra was shown for the Ir-containing boron-rich τ -boride $Co_{12.3}Ir_{8.9}B_{10.5}$ [4]. Our results for $Ni_{12.3}Ir_{8.7}B_{10.4}$ are perfectly in line with these observations.

According to the refinement iridium shows a clear preference of the site *M1* (84%), but *M2* contains significant amounts of Ir, too (18%). This leads to an enlargement of the *M*–B distances (2.19–2.20 Å) in comparison to other binary and ternary Ni borides. Furthermore, the sites *M3* and *M4* are only partially occupied. This was already observed for $Cr_{7.9}Ir_{14.1}B_6$ and $Co_{12.3}Ir_{8.9}B_{10.5}$. As a result the distances *M3*–*M1* are quite short despite the enlarged lattice parameter. Finally, the uptake of additional boron is evident. The distances *M*–B (2.186 Å) and B–B (1.69 Å) are comparable to the values in related compounds. In total, the results are very similar to the boron-rich τ -boride of the system Co/Ir/B.

4. Conclusions

The cubic τ -borides $Ni_{23-x}M'_xM''_yB_{6+4y}$ with $M'=Zn, Ga, In, Sn$, Ir were synthesised from the elements. On the basis of single crystal data detailed statements on the existence of boron rich phases and the arrangement of M' were possible. It could be shown the substitution of metal atoms by B_4 -tetrahedra on one of the metal sites (8c) is a common feature for Ni-containing τ -borides. For $M'=Zn$ and Sn the extent of substitution is limited (up to 20%), while for $M'=Ga$ there is a complete substitution $Ga \leftrightarrow B_4$ similar to the system Ni/Al/B. No additional boron was observed for $M'=In$, but there is an unexpected pattern of substitution. This might be explained by a miscibility gap of the

metallic melt. Iridium as a τ -stabiliser plays a special role. There exists only a boron-rich boride and Ni and Ir are in nearly equal ratios. Detailed investigations were done for a single crystal with a composition $\text{Ni}_{12.3}\text{Ir}_{8.7}\text{B}_{10.4}$. Iridium is mainly localised on site 32f. The 8c-site is occupied by 60% with B_4 -tetrahedra.

5. Note in addition

During the preparation of this article Sologub et al. [36] reported on single crystal investigations on the τ -borides $(\text{Co}_{0.64}\text{Ir}_{0.36})_{21}\text{Co}_{0.16}\text{B}_4\text{B}_6$ (i.e. $\text{Co}_{13.6}\text{Ir}_{7.6}\text{B}_{10}$) and $(\text{Fe}_{0.54}\text{Ir}_{0.46})_{20}\text{Fe}_3\text{B}_6$ (i.e. $\text{Fe}_{13.8}\text{Ir}_{9.2}\text{B}_6$). For the boron-poor phase $\text{Fe}_{13.8}\text{Ir}_{9.2}\text{B}_6$ they confirmed the mixed Fe/Ir occupation of the sites 48h and 32f with a preference of 32f as we have found it for $\text{Cr}_{7.9}\text{Ir}_{14.1}\text{B}_6$ [7] and $\text{Co}_{16.2}\text{Ir}_{6.8}\text{B}_6$ [4]. For the boron-rich phase $\text{Co}_{13.6}\text{Ir}_{7.6}\text{B}_{10}$ describes the structure with a model in space group $F\bar{4}3m$. The essential difference between the two models is a splitting of the site 8c in $Fm\bar{3}m$ into two independent fourfold sites in $F\bar{4}3m$. One of these two positions is completely occupied by B_4 -tetrahedra, the other one partially by Co (16%).

According to our experience this model has some shortcomings. The displacement parameter of the two independent boron atoms differ by a factor of 20 ($U_{\text{iso}} \text{B1}: 0.0039(12), \text{B2}: 0.0002(15)$). In comparison to our results, an early report on $\text{Co}_{21}\text{Ta}_2\text{B}_6$ [37], the already mentioned $\text{Ni}_{21}\text{In}_2\text{B}_6$ [16], and to recent findings of Gumeniuk et al. [38] on $\text{Ni}_{21}\text{Sc}_2\text{B}_6$ and $\text{Ni}_{21}\text{Zr}_2\text{B}_6$ and the rare-earth representatives $\text{RE}_{2-x}\text{Ni}_{21}\text{B}_6$ ($\text{RE}=\text{Er}, \text{Yb}, \text{Lu}$) [39] the value for B2 is unreasonably small. Additionally, there is no significant shift of the metal atom on site 48h $x,x,0$, which is severely involved in the surrounding of the site 8c in $Fm\bar{3}m$. Therefore there are no significant differences between the structure models except the splitting of the 8c-site ($Fm\bar{3}m$) in 4c and 4d ($F\bar{4}3m$). The only partial occupation of 4c by Co and the unusually small displacement parameter of B2 on 4d suggest that the occupation factor of B2 is higher and the description of structure in $F\bar{4}3m$ instead of $Fm\bar{3}m$ is not really validated by the X-ray data. The refinement of our data of boron-rich crystals with the model of Rogl did not result in a significant improvement. Nevertheless, the data of Rogl et al. clearly confirm the existence of a boron-rich τ -boride $\text{Co}_{13.6}\text{Ir}_{7.6}\text{B}_{10}$ and the substitution of M3 on site 8c by B_4 -tetrahedra as it was earlier proposed [4].

References

- [1] P. Villars, in: Pearson's Handbook, Crystallographic Data for Intermetallic Phases, ASM International, Materials Park, OH, 1997;

- P. Villars, K. Cenzual, in: Pearson's Crystal Data: Crystal Structure Database for Inorganic Compounds, ASM International, Materials Park, Ohio, USA, 2009/2010 Release.
- [2] A. Westgren, Jernkontorets Ann. 117 (1930) 501–512.
- [3] H.H. Stadelmaier, Metal-rich metall-metalloid phases, in: B.C. Giessen (Ed.), Developments in the Structural Chemistry of Alloy Phases, first ed., Plenum Press, New York 1969, pp. 141–180.
- [4] D. Kotzott, M. Ade, H. Hillebrecht, J. Solid State Chem. 182 (2009) 538–546.
- [5] P. Rogl, H. Nowotny, Monatsh. Chem. 104 (1973) 1325–1332.
- [6] H. Hillebrecht, M. Ade, Angew. Chem. 110 (1998) 981–983 Angew. Chem. Int. Ed. 37 (1998) 935–938.
- [7] D. Kotzott, M. Ade, H. Hillebrecht, Solid State Sci. 10 (2008) 2921–302.
- [8] D. Kotzott, Diploma Thesis, Universität Freiburg, Germany, 2006.
- [9] M. Ade, Ph.D. Thesis, Universität Freiburg, Germany, 1997.
- [10] Fa. STOE, programme XSHAPE, part of programme XAREA, Darmstadt, Germany, 2004.
- [11] N. Vojteer, H. Hillebrecht, Angew. Chem. 118 (2006) 172–175 Angew. Chem. Int. Ed. 45 (2006) 165–168.
- [12] T. Ludwig, H. Hillebrecht, J. Solid State Chem. 179 (2006) 1623–1629.
- [13] V. Adasch, K.-U. Hess, T. Ludwig, N. Vojteer, H. Hillebrecht, Chem. Eur. J. 13 (2007) 3450–3458.
- [14] M. Ade, D. Kotzott, H. Hillebrecht, J. Solid State Chem, in press, doi:jsscc.2010.05.009.
- [15] (a) G.M. Sheldrick, in: Programme SHELXL, University of Göttingen, Germany, 1997;
- (b) G.M. Sheldrick, Acta Crystallogr. A 64 (2008) 112–122.
- [16] T. Adelsberger, M. Jansen, Z. Anorg. Allg. Chem. 625 (1999) 438–442.
- [17] U. Müller, in: Anorganische Strukturchemie, Teubner-Verlag, 2006.
- [18] H.H. Stadelmaier, M.-L. Fiedler, Z. Metallkd. 60 (1969) 447–448.
- [19] N.F. Chaban, Y.B. Kuzma, Dopov Akad. Nauk Ukr. RSR (Ser. A) (1973) 550 cited from [1].
- [20] M. Atoji, W. Libscomb, Acta Crystallogr. 6 (1953) 547–550.
- [21] D. Thierry, Ph.D. Thesis, University of Stuttgart 1992.
- [22] T. Mennecke, P. Paetzold, R. Boese, D. Blaser, Angew. Chem. 103 (1991) 199–201 Angew. Chem. Int. Ed. Engl. 30 (1991) 172–174.
- [23] H.H. Stadelmaier, J.-D. Schöbel, L.T. Jordan, Z. Metallkd. 16 (1962) 752–754.
- [24] H.H. Stadelmaier, R.A. Draughn, G. Hofer, Z. Metallkd. 54 (1963) 640–644.
- [25] H.H. Stadelmaier, L.T. Jordan, Z. Metallkd. 53 (1962) 719–721.
- [26] H.H. Stadelmaier, J.B. Balance, Z. Metallkd. 58 (1967) 449–451.
- [27] J.-D. Schöbel, H.H. Stadelmaier, Z. Metallkd. 55 (1964) 378–382.
- [28] H.H. Stadelmaier, T.S. Yun, Z. Metallkd. 53 (1962) 754–756.
- [29] J.-D. Schöbel, H.H. Stadelmaier, T.R. Smith, Metall. (Berlin) 25 (1971) 10–12.
- [30] L.T. Jordan, R.K. Mathur, K.R. Brose, H.H. Stadelmaier, Z. Metallkd. 72 (1981) 782–784.
- [31] E. Ganglberger, H. Nowotny, F. Benesovsky, Monatsh. Chem. 96 (1965) 1144–1146.
- [32] H. Okamoto, in: Phase Diagrams for Binary Alloys, ASM International, Materials Park, Ohio, 2000.
- [33] I.D. Brown, J. Appl. Cryst. 29 (1996) 479–480.
- [34] M. Ade, D. Kotzott, M. Robertson, H. Hillebrecht, Z. Kristallogr. Suppl. 20 (2006) 151.
- [35] E. Ganglberger, H. Nowotny, F. Benesovsky, Monatsh. Chem. 97 (1966) 101–102.
- [36] O. Sologub, P. Rogl, G. Giester, Intermetallics 18 (2010) 694–701.
- [37] H.H. Stadelmaier, H.H. Davis, H.K. Manatakla, E.T. Henig, Z. Metallkd. 80 (1989) 370–373.
- [38] R. Gumeniuk, Y. Prots, W. Schnelle, A. Leithe-Jasper, Z. Kristallogr. NCS 223 (2008) 327–328.
- [39] J. Veremchuk, R. Gumeniuk, Y. Prots, W. schnelle, U. Burkhardt, H. Rosner, Y. Kuzma, A. Leithe-Jasper, Solid State Sci. 11 (2009) 507–512.